

Examination of spliced telecommunication fibers of the NZDS-SMF type adjusted to wavelength division multiplexing

MAREK RATUSZEK, JACEK MAJEWSKI, ZBIGNIEW ZAKRZEWSKI, JÓZEF ZALEWSKI

Institute of Telecommunications, University of Technology and Agriculture in Bydgoszcz, al. Prof. S. Kaliskiego 7, 85–796 Bydgoszcz, Poland.

Measurements of NZDS-SMF fiber parameters of the TrueWave[®] and LEAF[™] type adjusted to wave multiplexing have been presented. The results of optimization of fibers splicing conditions have been shown, as well as measurements of loss and mechanical strength of non-optimized and optimized splices. The calculation results of diffusion coefficient of GeO₂ dopant diffusing from the core to the cladding during the splicing process are also presented.

1. Introduction

In single channel systems as well as in multiple channel systems effects occur which have not attracted much attention until recently: optical nonlinear effects in glass. For Wave Division Multiplexing (WDM) systems which are used more and more nowadays the most destructive one is Four-Wave Mixing (FWM) which leads to channel crosstalk [1]. The FWM can be suppressed by dispersion – the more, the better. This has consequences for the application of fibers in the WDM system. The FWM is generated by the dependence of refractive index on light power density, and causes generation of additional spectrum components. The additional components are generated at frequencies $2f_1 - f_2$ and $2f_2 - f_1$ for two channels with frequencies f_1 and f_2 . In the case of a higher number of channels there will be, accordingly, more components [2].

The effectiveness of the FWM decreases with the spacing of channels and the dispersion coefficient D increases. A high dispersion characteristic of the fiber causes a significant differentiation of propagating wave group velocities, which reduces phase adjustment, and in effect decreases the efficiency of generation of waves with new frequencies [3]. It means that the standard Single Mode Fibers (SMF), [4] with zero dispersion in the second optical window (Fig. 1) fulfil the conditions very well, even for Dense Wavelength Division Multiplexing (DWDM) in the third optical window. In the third optical window, in the operating range of Erbium Doped Fiber Amplifiers (EDFA) where multiwave transmission WDM is possible for $\lambda = 1530 - 1565$ nm, $D \approx 18$ ps/nm·km for standard SMF is anticipated. On the other hand, fibers with dispersion shifted DS-SMF [5] have their operating range

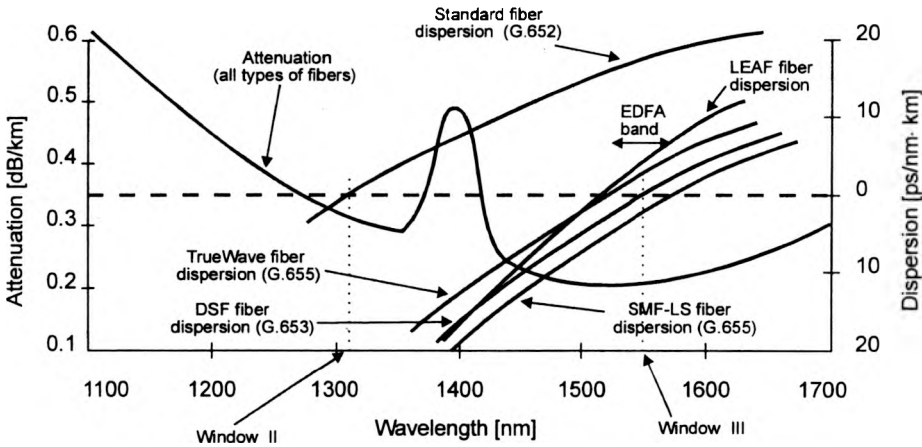


Fig. 1. Attenuation and dispersion of fibers of different types.

EDFA $D \approx 0$ ps/nm·km, which supports occurrence of the FWM. However, a big dispersion in the third window of standard SMF, $D \approx 18$ ps/nm·km, limits transmission rate. Expansion of the impulse Δt is related to the light source spectrum line width $\Delta\lambda$ and to the fiber length L by the equation [2]

$$\Delta t = D \cdot \Delta\lambda \cdot L. \quad (1)$$

The values of D and L are determined for a given route. The value of $\Delta\lambda$ cannot be reduced to zero. It is limited by the modulation information band. Due to this fundamental limitation it is not possible to obtain transforming distances, for transmission rate $B = 10$ Gbit/s for standard SMF, longer than 50–60 km.

Thus, when transmitting WDM and DWDM over very long distances with the use of EDFA amplifiers, use is made of single mode fibers with not high, but definitely non-zero dispersion (plus or minus), which are called NZDS-SMF (Non Zero Dispersion Shifted-Single-Mode Fiber), [6]. Examination of the splices of NZDS-SMF fibers as well as NZDS-SMF and standard SMF fibers is the aim of this work.

2. Parameters and measurement of NZDS-SMF fibers

At present four types of NZDS-SMF (Fig. 1) telecommunication fibers are being used in practice. These are:

1. TrueWave[®](+) – with positive dispersion in the range 1530–1565 nm (Lucent Technologies).
2. TrueWave[®](-) – with negative dispersion in the range 1530–1565 nm (Lucent Technologies).
3. LSTM – with negative dispersion in the range 1530–1565 nm (Corning).
4. LEAFTM – with positive dispersion in the range 1530–1565 nm and bigger effective area A_{eff} (Corning).

The parameters of three out of the above mentioned fibers, and their comparison with standard SMF 1528 [7], [8] are shown in Tab. 1.

Table 1. Different fibers used at transmission wavelength between 1530 and 1565 nm

	Standard SMF 1528 (OVD)	TrueWave®+ (MCVD)	LS™ (OVD)	LEAF™ (OVD)
Attenuation at 1550 nm [dB/km]	0.19 ÷ 0.23	0.21 ÷ 0.25	0.21 ÷ 0.25	0.21 ÷ 0.25
Dispersion at 1530 ÷ 1565 nm $\left[\frac{\text{ps}}{\text{nm} \cdot \text{km}} \right]$	$D \approx 18$	0.8 ÷ 4.6	$0 > D \geq -3.5$ (1530 ÷ 1560)	0.8 ÷ 6.0
λ_0 [nm]	1310	< 1530	> 1560	< 1530
Refractive index profile				
Mode field diameter at 1550 nm [μm]	≈ 10.5	≈ 8.4	≈ 8.4	9.0 ÷ 10.0
A_{eff} [μm ²]	80	≈ 55	55	≈ 72
Nonlinear refractive index $n_2 \cdot 10^{-20}$ [m ² /W]	2.2	-	2.3	2.3
Nonlinear coefficient $n_2/A_{\text{eff}} \cdot 10^{-9}$ [1/W]	0.27	-	0.42	0.32
Numerical aperture	≈ 0.13	≈ 0.15	0.16	≈ 0.12
Core diameter [μm]	≈ 8.5	≈ 5.5	≈ 6	≈ 7

In this table, OVD and MCVD indicate the type of fiber technology, and the values of fiber numerical apertures are estimated. The nonlinearity of glass materials is described by the Kerr constant, also called nonlinear refractive index n_2 . It is related to the refractive index n by

$$n = n(\omega) + n_2 \frac{P}{A_{\text{eff}}}, \quad (2)$$

$n(\omega)$ accounts for dispersion, depending on the frequency of light. The power P of the light pulse and the area over which the power is distributed in the fiber, A_{eff} mediate nonlinear effects. The LEAF™ fiber is a non-zero dispersion-shifted fiber with a large effective area which reduces the nonlinear coefficient in comparison to other dispersion shifted fibers (LS™, True Wave®).

2.1. Measurements of TrueWave® and LEAF™ fibers

Catalogue parameters of TrueWave® and LEAF™ fibers have been verified by measuring their parameters. Besides, precise knowledge of the parameters such as numerical aperture, mode field diameter, core diameter, refractive index profile is indispensable in optimization of the fiber splicing process. For verification of the catalogue parameters, measurement systems Model 2400 and 2500, Photon Kinetics,

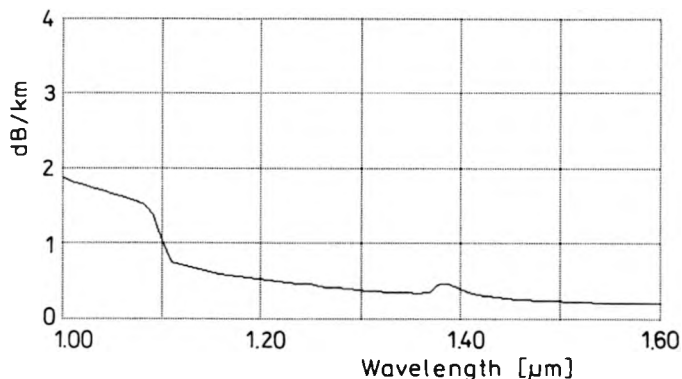


Fig. 2. Run of the TrueWave[®] fiber attenuation $\alpha_{1310} = 0.375$ dB/km, $\alpha_{1550} = 0.213$ (± 3 nm resolution power).

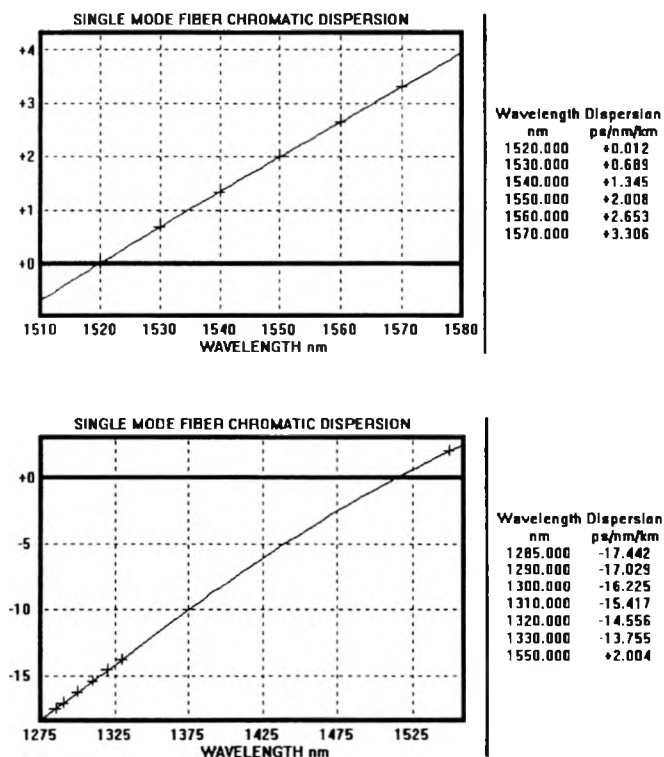


Fig. 3. TrueWave[®] fiber dispersion.

were used as well as Model CD 300 of the firm EG&G in the case of dispersion measurement. Measurements of fiber parameters with the use of these systems are based on methods recommended by ITU-T [4].

The following parameters for particular fibers were obtained from measurements:

TrueWave[®] fiber:

- spectral attenuation (Fig. 2),
- dispersion (Fig. 3),
- mode field diameter (Tab. 2),
- numerical aperture (calculated), $NA = 0.154$,
- cut-off wavelength in the fiber $\lambda_c = 1131.63$ nm,
- core diameter $2a = 5.62$ nm,
- core radiation intensity profile (Fig. 4).

LEAF[™] fiber:

- attenuation $\alpha_{1550} = 0.203$ dB/km,
- dispersion $D_{1535} = 1.908 \frac{\text{ps}}{\text{nm} \cdot \text{km}}$, $D_{1565} = 4.902 \frac{\text{ps}}{\text{nm} \cdot \text{km}}$,
- mode field diameter (Peterman II) $MFD_{1550} = 10.16$ μm ,
- cut-off wavelength in the fiber $\lambda_c = 1503$ nm,
- core radiation intensity profile (Fig. 5).

The measurement results confirm catalogue data within the limit accuracy.

3. Examination of NZDS-SMF fiber splices

In examinations of splices, TrueWave[®](+) and LEAF[™] have been used, as well as six types of standard fibers of various makes manufactured according to MCVD (Modified Chemical Vapour Deposition), OVD (Outside Vapour Deposition) and VAD (Vapour Axial Deposition) technologies, in all connection combinations.

Splicing fibers NZDS-SMF and standard SMF ones despite differences in numerical apertures, that is, differences in core GeO₂ dopant concentrations, profile of refractive index and mode field diameters can certainly be used because a few kilometer-distances of standard SMF do not affect negatively WDM transmission systems with use of NZDS-SFM.

Splices were produced by a fusion splicer Ericsson FSU-925 after modifying, according to the fiber types, its three-step splicing process. Splice loss measurements were performed with the use of OTDR method in two directions, for $\lambda = 1310$ and 1550 μm .

3.1. OTDR splice loss measurements

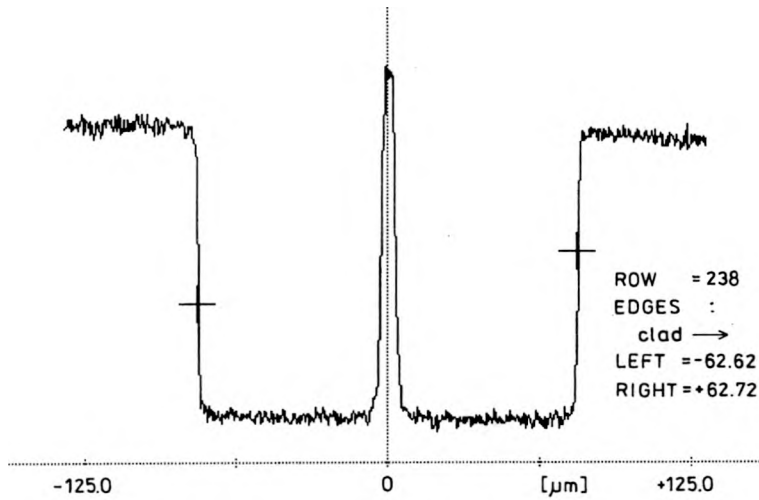
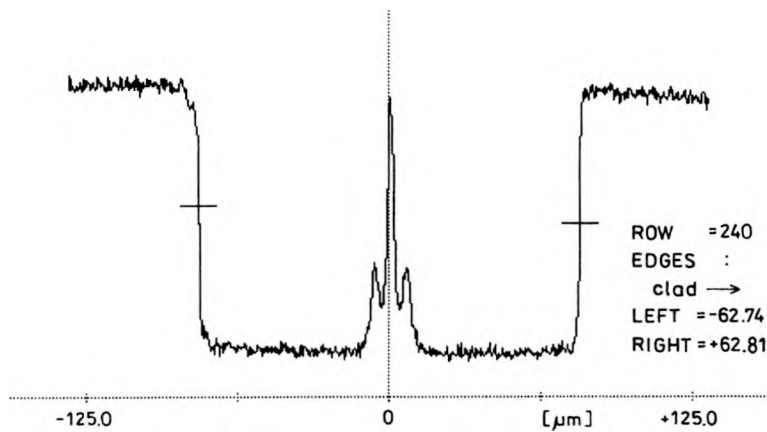
The OTDR is now commonly used to estimate splices loss for single-mode fibers. According to [9], the backscattered power detected by OTDR from a point immediately preceding the splice is given by

$$P_1 = P_0 S_1 \exp(-2\alpha_1 L_1) \quad (3)$$

where P_0 is the initial power level, L_1 – the fiber length, α_1 – the attenuation coefficient, and S_1 – the capture fraction, the latter being given by [10]

Table 2. Mode field diameter (Peterman II) MFD

λ [nm]	MFD [μm]
1200	6.0961
1300	6.6415
1500	7.8813
1550	8.2405
1600	8.6193

Fig. 4. Core radiation intensity profile in TrueWave[®] fiber.Fig. 5. Core radiation intensity profile in LEAF[™] fiber.

$$S_1 = 0.038 \left(\frac{\lambda}{n_1 w_1} \right)^2 \quad (4)$$

where λ is the wavelength, w_1 and n_1 – the mode field radius and the core refractive index, respectively. The subscript 1 refers to the input fiber.

The backscattered power detected by OTDR from a point immediately following the splice is given by [9]

$$P_2 = P_0 S_2 T_{12} T_{21} \exp(-2\alpha_1 L_1) \quad (5)$$

where T_{12} is the splice transmission value in the forward direction, and T_{21} – the corresponding quantity in the reverse direction. The capture fraction S_2 is given by

$$S_2 = 0.038 \left(\frac{\lambda}{n_2 w_2} \right)^2 \quad (6)$$

where the subscript 2 refers to the output fiber.

The one-way OTDR splice result is determined from the ratio of these two power levels

$$\alpha_{12} = 20 \log \left[\frac{1}{2} \left(\frac{w_1}{w_2} + \frac{w_2}{w_1} \right) \right] + 10 \log \frac{w_2}{w_1} + 10 \log \frac{n_2}{n_1} \quad (7)$$

In Equation (7) the first term describes the true splice loss caused by MFD mismatch, the second and third terms imply the apparent losses due to MFD and refractive index mismatch of the two fibers, respectively.

From Equation (7) the one-way splice loss obtained via OTDR technique is equal to the true splice loss plus two apparent losses. Therefore the contribution of the third term can be neglected because of its value being much smaller compared to that of the second term. As the absolute value of the second term may be much larger than the true splice loss, a one-way OTDR result may exceed the splice loss by far, or even turn into an apparent gain. Similarly, the one-way OTDR value when measured from the opposite direction is given by

$$\alpha_{21} = 20 \log \left[\frac{1}{2} \left(\frac{w_1}{w_2} + \frac{w_2}{w_1} \right) \right] + 10 \log \frac{w_1}{w_2} + 10 \log \frac{n_1}{n_2} \quad (8)$$

Obviously, the true splice loss is obtained by averaging Eqs. (6) and (7)

$$\alpha_s = 20 \log \left[\frac{1}{2} \left(\frac{w_1}{w_2} + \frac{w_2}{w_1} \right) \right] \quad (9)$$

3.2. Loss of NZDS-SMF fiber splices

Spliced connections of fibers of the TrueWave[®]–TrueWave[®] and LEAF[™]–LEAF[™] type are performed easily with the use of splicing programs for standard SMF. The above mentioned losses of splices are observed for both $\lambda = 1310$ and 1550 nm with values $\alpha_s < 0.08$ dB in a repeatable way. However, the TrueWave[®]

–LEAFTM TrueWave[®] standard SMF and LEAFTM–standard SMF splices require optimization process.

Without optimization in three steps of the splicing process the splice loss of the above mentioned splice combination ranges from 0.15 to 0.3 dB, and is considerably higher than the expected values in telecommunication fiber links. It should be emphasized, though, that losses of LEAFTM splices with standard SMF are in the lower limit of the above range.

3.3. Optimization of NZDS-SMF fiber splicing process

Splices with small loss and good optical return loss are obtained when, due to proper migration area of doping in cores and clades which are being connected, a proper intermediate area (redistribution dopant) is obtained [11], [12], Fig. 6. Obtaining optimal intermediate area is a function of time and splicing current in the three steps of splicing – FSU-925 RTC (Tab. 3).

Exemplary microscopic pictures of non-optimized splices are shown in Fig. 7.

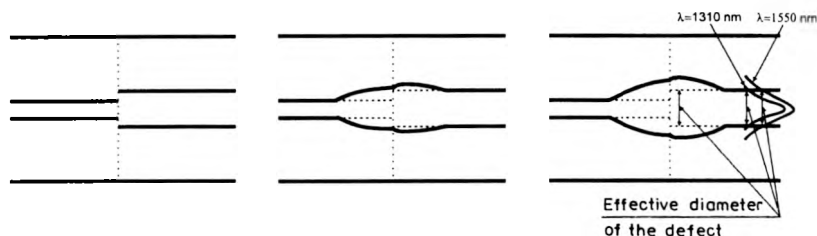


Fig. 6. Schematic presentation of doping migration area –intermediate area.

Table 3. Results of reflectometric measurement of splice loss (mean value from minimum three splicing tests, optimized program, fusion splicer FSU-925 RTC)

		SMF Siecor (OVD)	SMF AT&T (MCVD)	SMF Fujikura (VAD)	SMF Optical Fibres	TrueWave
		dB	DB	DB	dB	dB
λ = 1310 nm	TrueWave	0.05	0.04	0.06	0.04	
	LEAF	0.08	0.08	0.08	-	0.06
λ = 1550 nm	TrueWave	0.05	0.02	0.05	0.04	
	LEAF	0.06	0.05	0.06	-	0.035

3.4. Loss measurement of optimized splices

When the core diameters and numerical apertures of spliced fibers are comparable, the splice loss is higher for λ = 1550 nm than for λ = 1310 nm. This results from

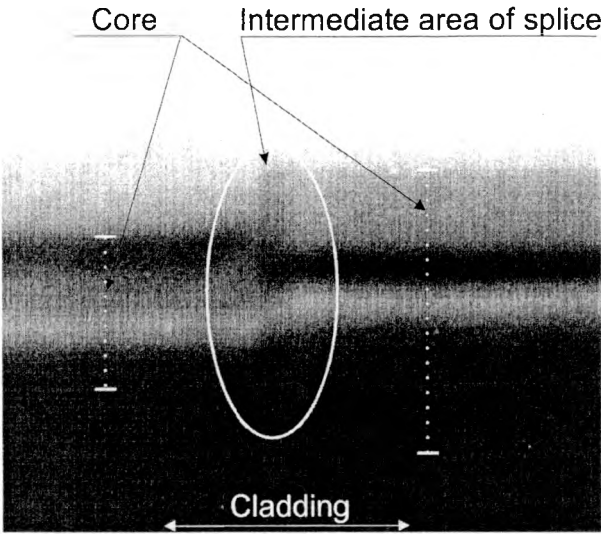


Fig. 7. Microscopic picture of a splice without optimization, the left core of TrueWave[®] and the right core of SMF Lycom.

a bigger mode field diameter for $\lambda = 1550$ nm. It means that the defect field, *i.e.*, the splice, is larger for $\lambda = 1550$ nm, which causes a bigger loss of optical power. This phenomenon is not explicitly accounted for in Eq. (9).

On the other hand, loss of fiber splices which differs significantly with core diameters and numerical apertures shows higher values for $\lambda = 1310$ nm than for $\lambda = 1550$ nm. This refers mainly to non-optimized splices. For optimized splices these differences are smaller (Tab. 3). An opposite dependence of the splice loss on the wavelength λ , for fibers which differ significantly in core diameters and numerical apertures, proves, in our opinion, that the effective field of the defect, *i.e.*, the splice has been reduced for $\lambda = 1550$ nm, that is for a bigger MFD mode field than in the case of $\lambda = 1310$ nm (Fig. 6). Assuming the dopant diffusion within the splice (Fig. 6), for the optimized splices with higher dopant diffusion it means exclusion of the cladding from the defect field and the reduction of the splice loss for $\lambda = 1550$ nm. The results of splice loss measurements using one-way OTDR confirm significant dopant diffusion during the splicing process. Fibers spliced at longer times and with higher splicing currents lower one-way show lower one-way losses. This means equalisation of the refractive index values n_1 and n_2 and mode field diameters $2w_1$, $2w_2$ in intermediate area of splicing fibers as well (Eqs. (7), (8), Fig. 6)).

We should emphasize that in the future OTDR measurements of splice losses will be modified by two-point measurements of transmission.

3.5. Measurements of splice mechanical strength

Measurements have been performed for all combinations of splices, for optimized and non-optimized ones (Fig. 8). The Ericsson tensile testing machine EFR 100 was

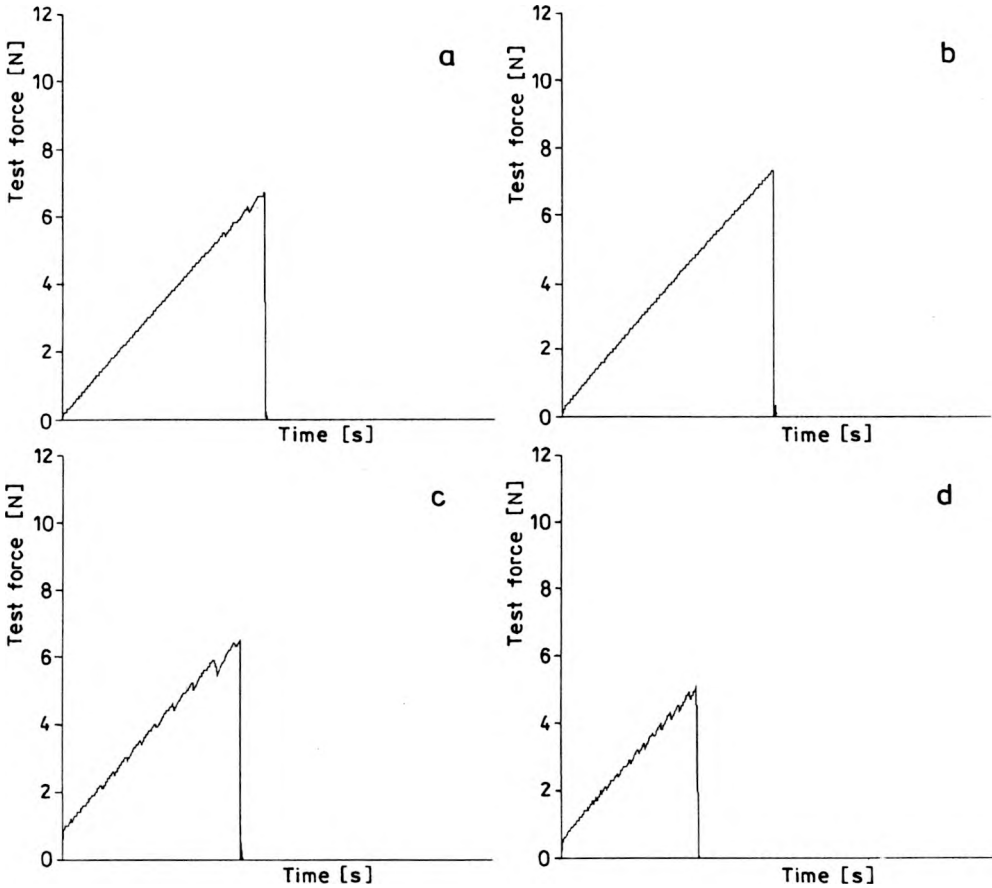


Fig. 8. Splice mechanical strength. a – TrueWave-SM Siecor (standard splicing), b – TrueWave-SM Siecor (optimized splicing), c – TrueWave-SM Lycom (standard splicing), d – True Wave-SM Lycom (optimized splicing).

used for the examinations. Optimization of splicing conditions does not decrease the mechanical strength of splices (strength of all > 5 N) which proves to show the structure continuity and lack of inclusions other than the amorphous structure.

4. Diffusion of GeO_2 in SiO_2 during splicing

In order to evaluate the diffusion processes GeO_2 , a single-mode fiber with $\text{NA} = 0.217$ and content of GeO_2 in the core of $C_{\text{GeO}_2} = 10.4\%$ mol/mol, and a quartz rod of $\sim 130 \mu\text{m}$ in diameter were used. Diffusion coefficients were calculated on the basis of changes, along splices, of thermoluminescence profiles of the above mentioned spliced fibers. The splice temperature was $2000 \text{ }^\circ\text{C}$ [13]. The time of the second step of splicing was changed from 1 to 6 s (Fig. 9). A linear dependence of thermoluminescence on GeO_2 concentration in SiO_2 was assumed

[14]. Curves of thermoluminescence intensity changes for different splicing times as a function of the distance from the splice front are shown in Fig. 10, [12], [13].

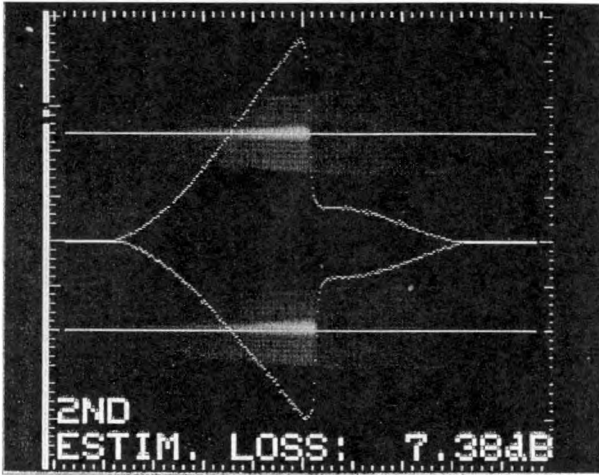


Fig. 9. Exemplary thermoluminescence intensity profile for $t = 6$ s.

For the purpose of calculation of the diffusion coefficient the following conditions and parameters have been assumed:

- diffusion from unlimited dopant source, *i.e.*, $N(0, t) = N_0$,
- initial concentration inside the quartz rod is small in comparison with N_0 .

Thus, GeO_2 concentration in the quartz rod may be rendered by the following expression:

$$N(x, t) = N_0 \operatorname{erfc} \frac{x}{2\sqrt{Dt}}. \quad (10)$$

Density of SiO_2 has been assumed as $\rho = 2.20 \text{ g/cm}^3$. The content $C_{\text{GeO}_2} = 10.4\% \text{ mol/mol}$ corresponds with the concentration of GeO_2 in SiO_2 : $N_0 = 2.27 \cdot 10^{21} \text{ cm}^{-3}$. With N_0 , x , t being known and $N(x, t)$ evaluated on the basis of luminescence, the values of diffusion coefficients D have been estimated for germanium in SiO_2 at the temperature $\approx 2000 \text{ }^\circ\text{C}$. The coefficients were calculated for the distances $x = 7.5 \text{ }\mu\text{m}$ and $x = 12.5 \text{ }\mu\text{m}$ from the splice front. The values obtained were found to change in the range $D = 3 \cdot 10^{-7} - 2 \cdot 10^{-6} \text{ cm}^2/\text{s}$. Higher coefficient values were obtained for shorter splicing times and smaller distances from the splice front. Dopant diffusion coefficients can be rendered by the following equation [15]:

$$D = D_\infty \exp\left(\frac{-E_a}{kT}\right) \quad (11)$$

where: D_∞ – diffusion coefficient for $T = \infty$, E_a – dopant activation energy in SiO_2 .

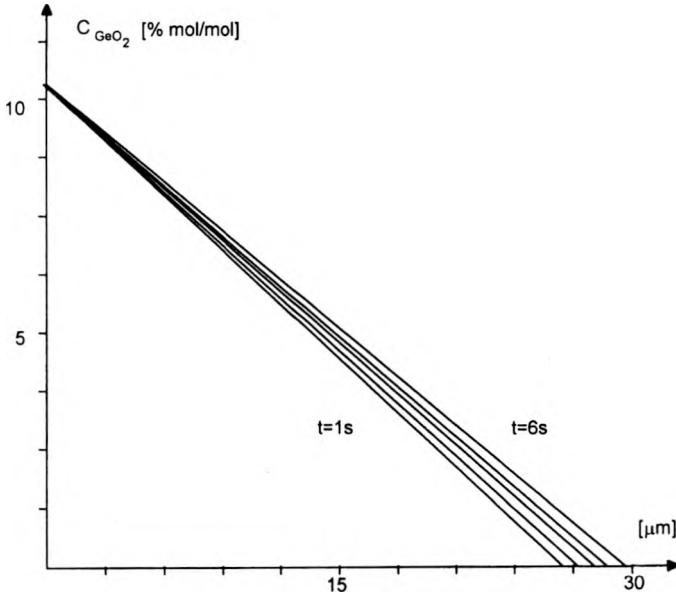


Fig. 10. Thermoluminescence intensity changes and assignment of GeO_2 in SiO_2 concentration for different splicing times at a distance from the splice front function

Having accepted theoretical values E_a [12], [15] for interatomic dopants $E_{aI} \approx 1$ eV and diffusing dopants by means of substituting $E_{aS} = 3.0$ eV, values of D_∞ were calculated. For E_{aS} : $D_\infty = 20 - 130$ cm^2/s , for E_{aI} : $D_\infty = 1.2 \cdot 10^{-4} - 8 \cdot 10^{-4}$ cm^2/s . The calculated values D_∞ for E_{aI} are close to the theoretical value $D_\infty = 1.7 \cdot 10^{-3}$ cm^2/s [15].

In the literature, there is no information about values of diffusion coefficient GeO_2 in SiO_2 at temperature 2000 $^\circ\text{C}$. Theoretically foreseeable diffusion coefficient for interatomic dopants in SiO_2 for temperature 1000 $^\circ\text{C}$ is $D = 4.1 \cdot 10^{-7}$ cm^2/s [15]. Using Eq. (11) theoretical value of diffusion coefficient at 2000 $^\circ\text{C}$ is $D = 2.6 \cdot 10^{-5}$ cm^2/s and it is higher than estimated value of diffusion coefficient in this paper.

5. Conclusion

The NZDS-SMF fibers of one type can be spliced with the use of standard splicing programs designed for standard SMF fibers. Due to differences in core diameters, numerical apertures and refractive indices, the splicing of different types of NZDS-SMF as well as NZDS-SMF fibers with SMF standard fibers requires optimization. Optimization means changing parameters of the three-step splicing process in order to obtain diffusion of the GeO_2 dopant from the core to the cladding of the spliced fiber such that the migration area can be formed, in which mismatches between refractive indices and core diameters of the spliced fibers will disappear.

Acknowledgements – The work was financed by a grant of the State Committee for Scientific Research No. 8T11D00613.

References

- [1] WIDEMAN G. F., WENSTEIN C., J. *Lightwave Technol.* **12** (1995), 40.
- [2] CHRAPLIVY A. R., *Nonlinear Effects in Optical Fibers*, Academic Press, San Diego, California, 1991.
- [3] AGRAWAL G. P., *Nonlinear Fiber Optics*, Academic Press, San Diego, California, 1989.
- [4] ITU-T G.652, *Characteristics of a single mode optical fiber cable*, 1994.
- [5] ITU-T G.653, *Characteristics of a dispersion-shifted single-mode optical fiber cable*, 1997.
- [6] ITU-T G.655, *Characteristics of a non-zero dispersion shifted single-mode optical fiber cable*, 1996.
- [7] *Fiber Focus* – Corning Materials, 1998.
- [8] TrueWave[®] Singlemode Optical Fiber – Lucent Technologies Materials, 1998.
- [9] MILLER C. M., METTER S. C., WHITE I. A., *Optical Fiber Splices and Connectors*, Marcel Dekker Inc., New York, Basel 1986.
- [10] NEUMANN E. G., *Single-Mode Fibers*, Springer-Verlag, Berlin 1988.
- [11] ZHENG W., *The Real Time Control Technique for Erbium Doped Fiber Splicing*, Ericsson Review, Sweden – Sundbyberg, 1993, pp. 1–24.
- [12] RATUSZEK M., ZAKRZEWSKI Z., MAJEWSKI J., ZALEWSKI J., *Problemy spawania jednomodowych, telekomunikacyjnych włókien światłowodowych stosowanych w Polsce i pochodzących od różnych producentów*, (in Polish), [In] Krajowe Sympozjum Telekomunikacji KST'97, Wydawnictwo Politechniki Warszawskiej, Vol. 3, 1997, p. 397.
- [13] Fusion Splicer FSU 925 RTC, User's Manual, Ericsson, 1992.
- [14] JOST W., *Diffusion in Solids, Liquids, Gases*, Academic Press, New York 1960.
- [15] WOLF H. F., *Silicon Semiconductor Data*, Pergamon Press, Oxford 1969.

*Received October 16, 1998
in revised form December 3, 1998*